Power and Energy Constrained Battery Operating Regimes: Effect of Temporal Resolution on Peak Shaving by Battery Energy Storage Systems

Shiyi Liu,[1] Sushil Silwal,[1] and Jan Kleissl[1]

Center for Energy Research, University of California San Diego

Battery Energy Storage Systems (BESS) are often used for demand charge reduction through monthly peak shaving. However, during economic analysis in the feasibility stage, BESS are often sized and BESS revenue is quantified based on 1 hour load and/or solar output data for one year. To quantify the error in the demand charge from coarse-resolution modeling, the effect of two temporal resolutions, 15 min and 1 hour, on peak load reduction is compared across a battery ratings space defined by power capacity and energy capacity. A linear program of the system optimizes the peak of the net load and the associated demand charge assuming perfect forecasts. Based on the 15 min load profile of a particular day, a critical power (CP) and critical energy (CE) can be defined, yielding a critical point in the power-energy space. Based on the difference of demand charge (DoDC) across the two load profiles at different temporal resolution for a real building, the battery rating space is divided into three different regions: oversized region, power-constrained region, and energy-constrained region, which are separated by CP and CE. The DoDC in the power-constrained and energy-constrained regions is explained by time averaging effects and the load sequence at high resolution. In the power-constrained region of the battery rating space, the difference between the original 15 min peak and the 1 hour average peak persists in the optimized net load until the battery power capacity is sufficiently large. In the energy-constrained region, averaging may change the peak period duration, which depends on the sub-hourly sequence of the original load data. Through artificial load data and reordering of real load data, we demonstrate that the sequence effect causes energy-constrained batteries to underestimate peak shaving and demand charge reduction. Demand charge savings were especially sensitive to the BESS power capacity: for a ≈ 50 kW load, demand charge errors were up to \$53 for power-constrained batteries and were an order of magnitude smaller for energy constrained batteries. The power capacity of the battery should be carefully considered when interpreting results from optimizations at low resolutions.

I. INTRODUCTION

A. Motivation for demand charge management

Battery Energy Storage Systems (BESS) can mitigate the challenges caused by uncertainty and variability of renewable energy generation in hybrid renewable energy systems and contribute to CO_2 emission reductions. BESS are also critical to demand-side management for power end-users in microgrids. For example, BESS have become a popular solution for electricity cost reduction in commercial buildings through peak demand reduction and an associated reduction in demand charges. Largely owed to progress in technology and manufacturing in the last 5 years, the BESS costs have decreased dramatically. With many countries aiming to achieve sustainable power grids and reductions in carbon emissions, it is anticipated that BESS will be widely implemented in the near future.

There are two primary categories of existing BESS research: (i) utility side or "in front of the meter" applications and (ii) demand side or "behind the meter" applications[1]. In utility side applications, BESS can provide grid services to power systems with high levels of renewable penetration to decrease intermittency and disturbances[2,3]. However, this paper targets demand side applications. Peak demand shaving is a popular BESS application in demand side management (DSM). Most commercial and industrial end-users are charged two components in electricity billing, energy charges and demand charges. Energy charges are based on the total energy (kWh) consumed while demand charges are a function of the peak demand in any 15-minute period of the billing cycle (typically one month). Through appropriate scheduling of charging and discharging (i.e., a battery dispatch schedule), BESS can reduce the peak demand and, thus, achieve economic savings[4]. To reach these goals, building and microgrid optimization typically requires forecasts of both renewable generation and electricity demand or load. For example, minimizing the annual energy cost, the mixed-integer linear programming (MILP) DER-CAM model elucidated the drivers for adoption of BESS[4]. REopt[5] evaluates economic viability, identifies system sizes of grid connected PV, wind and battery systems, and provides an optimal BESS dispatch strategy.

B. Literature review on time resolution effects on modeling battery dispatch schedules

The temporal resolution of input data and models has significant impacts on simulation, design, and operation of energy systems including BESS. Bistline[6] cautions that while analyses performed with simplified temporal aggregation reduce computational cost, they cannot accurately evaluate the advantages of renewable generation or storage systems. Bistline also points to a need for higher data resolution for policy analysis, power system planning, and technology evaluation in scenarios with higher penetration of variable renewables. Similar conclusions are drawn by Abdullaha et al.[7] for residential BESS, Poncelet et al.[8] for energy system planning models, and by Jaszczur et al.[9] for energy flows between PV, home, and grid and self-consumption. Schmid et al.[10], Hack et al.[11], and Tang et al.[12] also confirm that higher resolution data results in better accuracy of techno-economic analyses of BESS.

Battery dispatch scheduling is sensitive to the time resolution (or time averaging; both are used synonymously here consistent with the literature) of the load profiles. Most analyses on temporal resolution use residential load profiles. However, since residential electricity tariffs are only volumetric and not a function of peak load, these analyses do not consider minimizing load peaks which is important for commercial customers in reducing demand charges. Peak shaving and valley filling is also important to grid operators in enhancing grid reliability, such as in analyses of BESS impacts on larger power systems using hourly load and generation data (Yang et al.[13]). Wright et al.[14] analyzed averaging effects on the import and export proportion of on-site generation for a residential load with time averaging ranging from 1 to 30 min. Longer averaging was unable to capture short-term peaks, reducing peak loads. Cao & Siren[15] analyzed the error of the fraction of production consumed on-site (also referred to as self-consumption ratio) and fraction of local demand supplied by PV (also referred to as self-sufficiency) as a function of time resolution. Coarser resolutions overestimated the self-consumption and self-sufficiency because the load variability decreased with averaging. Adding a BESS as in a PV+BESS (PVB) system reduced these errors significantly due to the ability to flatten spikes. Stenzel et al.[16] analyzed the impact of time resolution on self-consumption rates for PVB. Self-consumption was over-estimated for longer averaging times due to smoothing, leading to an overestimation of the cost-savings from PVB. Beck et al.[17] assessed the effect of temporal resolution of PV generation and electrical load ranging from 10 s to 60 min with a MILP model. A temporal resolution of 60 min was found to be sufficient for sizing both the PV and PVB systems. Especially for PVB, the influence of time resolution was negligible. Burgio et al.[18] studied the impact of time averaging and PVB system size on PVB system economics. Temporal averaging did not affect PVB sizing. However, a time resolution of 60-min caused a substantial under-estimation (39%) of the peak load, as compared to a 3 min resolution. Talavera et al.[19] proposed a new BESS sizing approach also considering nominal impacts of input data resolution. However, we will later show that around certain BESS power capacities, BESS sizing economics are very sensitive to and can be reduced by higher data resolution.

C. Research gap

Most of the research on the effect of temporal resolution targets self-consumption or self-sufficiency, which has been motivated by renewable feed-in policies, e.g. in Germany. Self-consumption is overestimated at coarse time resolutions, as the high-frequency variation of the load and solar profiles are averaged out. For BESS peak shaving and demand charge reduction, it is trivial that peak loads of PVB systems will be underestimated for low temporal resolutions. For example, in Burgio et al.[18] the peak of the 15 min load, 15 min load+PV, and 15 min PVB grid imports was 12%, 15%, and 15% higher than that of hourly load for one day, respectively (their Table 6). Burgio et al. is the only study that reported peak grid import values for PVB systems at different temporal resolutions, but did so in passing only. Burgio et al.[18] performed economic analysis of PVB systems on high-resolution electric load data for one day at a university laboratory and office building. While Burgio et al.[18] focused on analyzing self-consumption for hypothetical residential PVB systems and reported peak values only for a single day and a single PVB configuration, our study compares the DoDC for the entire power-energy space of the BESS for several days. In summary, the interaction of BESS properties, load shape, and temporal resolution have not yet been systematically quantified in the context of demand charge reduction.

D. Overview of the paper and hypothesis

The gap in the literature is addressed by examining the difference between optimal demand charges (DoDC; viz the net load peak) achieved by BESS dispatch scheduling based on load profiles for two common temporal resolutions, 15 min and 1 hour. Our hypothesis is that BESS dispatch modeling at 1 hour interval underestimates the actual demand charges for BESS that are too small in power rating, energy rating, or both. The 15 min interval is the benchmark as it is used by most utilities for customer metering, while the 1 hour interval is a more common resolution of solar resource data and is typically applied in optimization models to reduce computational cost (e.g.[5],[20]). We establish DoDC regimes (i.e. BESS benefits) within the BESS power-energy rating space based on several indicators. A critical point separates the power-energy rating space into three regions: (i) power-constrained, (ii) energy-constrained, and (iii) oversized region. The magnitude and trends of the DoDC are linked to the regions of the BESS space and the properties of the load timeseries.

E. Novelties

This is the first systematic analysis of the interaction of BESS properties, load shape, and temporal resolution for demand charge reduction. We identify for the first time how and by how much BESS power and energy ratings cause an underestimation of demand charges at a 1 hour temporal resolution compared to 15 min resolution.

F. Assumptions

We make several key assumptions: (i) We only consider non-coincidental demand charges (i.e. daily peaks), not peak demand charges. (ii) We only consider demand charges and not time-of-use energy charges. (iii) We optimize based on perfect forecasts. (iv) Power dynamics are not considered, which . While these assumptions are unrealistic and will distort the economic value of BESS, these choices are deliberate as the fundamental effect of BESS and load shape properties can be illustrated more clearly in the simplified electric tariffs and optimization inputs assumed here.

G. Structure of the paper

The rest of the paper is organized as follows: Section II reviews the methodology, Section III presents the results, and Section IV provides conclusions and future directions.

II. METHODOLOGY

A. Optimization Problem

To analyze the effect of temporal resolutions, a simple energy system is adopted consisting of three main components: (i) the utility grid, (ii) the load, and (iii) a BESS with adjustable

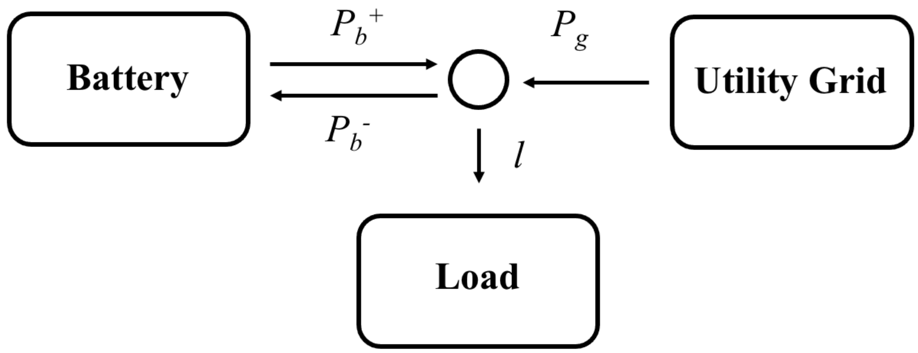

FIG. 1. Schematic of the power system including a BESS, load, and utility grid with power flows.

parameters (Fig. 1). All electronic converters, connections, and electric lines are assumed to be lossless and unlimited in capacity. The system is assumed to be grid-connected at all times. The analysis is limited to energy-matching; frequency voltage control, dynamics, as well as protection are handled by other systems or insignificant over time scales of minutes and are not of concern here. All of these assumptions are common in microgrid sizing and dispatch research[5,18–20]. The BESS is assumed to be 100% efficient.

To study the economic savings of the behind-the-meter BESS, the meter net load given by P_g is recorded. P_g measures electricity imported from the utility resulting from the original load, l, offset by the negative (charging) or positive (discharging) power from the BESS P_b, $P_g = l - P_b$. The BESS response is assumed to be instantaneous, such that the charging/discharging dispatch is "on demand". Given that the response time of Lithium-ion type batteries is on the order of milliseconds (i.e. much smaller than the time interval), this assumption is justified[1]. The charging/discharging power of BESS, P_b (kW), is limited by the nominal power capacity, c_p (kW), and energy capacity, c_e (kWh).

Without loss of generality, the load in this example is a true building load. But the same method can be applied to any time series, such as a net load resulting from summation of actual load and PV generation. Specifically, we are interested in the peak net load that determines the demand charge.

The optimization model is a convex optimization problem, which is formulated in discrete time with time step size, Δt, determined by the temporal resolution of the load profile. The optimization model minimizes an objective function J

$$\min \quad J = d \times \max(P_g) + \varepsilon \times \sum_{n=0}^{N} |P_b^n|, \tag{1}$$

where d is the demand charge rate, ε is a penalty factor, N is the number of time steps, and n is the time index.

The first term in the objective function measures the optimal demand charge (ODC). ODC is the product of the maximum net load, which is called optimal peak (OP (kW)), and the demand charge rate:

$$ODC = d \times \max(P_g) = d \times OP \tag{2}$$

The demand charge rate, $d = 20.62$ \$/kW, is included as a multiplier to demonstrate the economics of reducing the optimal peak; d is obtained from the AL-TOU rate schedule for >500 kW demand by the local utility San Diego Gas & Electric (SDG&E). This rate does not affect the generality of the results but is included for illustrative purposes.

The second term is a penalty for charging/discharging power decisions. Of the many possible solutions with equal objective function, the penalty term ensures that the solution with the least battery activity is selected. By multiplying in a small coefficient, $\varepsilon = 10^{-6}$, the optimization model diminishes the oscillation of P_b^n while simultaneously preserving the ODC, because the first term has a much heavier weight than this penalty term.

The constraints are:

$$\text{Energy balance:} \quad P_g^n = l^n - P_b^n, \qquad \forall n \in N \tag{3a}$$

$$\text{Power capacity:} \quad -c_p \leqslant P_g^n \leqslant c_p, \qquad \forall n \in N \tag{3b}$$

$$\text{State of charge:} \quad \mathrm{SOC^{n+1}} = \mathrm{SOC^{n}} - \frac{\mathrm{P_b^n \times \Delta t}}{\mathrm{c_e}}, \forall n \in N \tag{3c}$$

$$\text{Initial state:} \quad \mathrm{SOC^{1}} = \mathrm{SOC^{end}} = 0.5 \tag{3d}$$

where SOC is the state of charge of the BESS. Equation (3a) requires that, at each time step, the net load supplied by the grid must equal the building load demand l^n minus the BESS power, where positive P_b is defined as discharging. According to (3b), the power from the BESS is constrained by the power capacity; $P_b^n > 0$ indicates discharging the BESS, and $P_b^n < 0$ indicates charging. While the BESS is charging or discharging, SOC must be consistent with the BESS dispatch as stipulated in the (3c). Following a common assumption for daily time horizons, the BESS is further constrained to be half charged at both the beginning (0000 h) and end of the day (2400 h). This initial condition in (3d) avoids savings through net battery discharge that may penalize performance on subsequent days. Instead, the net charging/discharging energy after the simulation period, T, is zero. The model is built using CVX in MATLAB with the MOSEK solver.

B. Load data and difference of optimal demand charge (DoDC)

The 2019 load data collected on October 7, 13, and 23 from the Police building on the campus of the University of California, San Diego (UCSD) is analyzed. The data show typical variations for commercial buildings but do not limit the generality of the LP model. Although the demand charge is usually measured in billing cycles of one month, this study examines only one day at a time for illustrative purposes (i.e., $T = 24$ hours).

We consider two temporal resolutions of the input data: 15 min and 1 hour (i.e., 60 min). Since the load is measured as interval data of 15 min by the real SDG&E meter, 15 min is defined as the reference temporal resolution. On the other hand, many data sets, analyses, or optimization models for peak shaving are based on a 1 hour resolution (e.g., REopt). The low-resolution profile is derived by taking the average of four high-resolution time steps (Fig. 2). The number of battery dispatch decisions (i.e. number of time steps), N, for the same scheduling horizon, T for the 15 min resolution is 4 times that of the 1 hour resolution. For dispatch scheduling over one day, where $T = 24$ hours, the decision numbers are given by:

$$N_{1-\text{hour}} = \frac{T}{\Delta t_{1-\text{hour}}} = 24, \quad \text{and}$$
$$N_{15-\text{min}} = \frac{T}{\Delta t_{15-\text{min}}} = 96$$

The 1 hour averaged load data may result in a different objective function value compared to the original 15 min load profile, which subsequently leads to a different optimal peak and a different optimal demand charge (ODC). This deviation is defined as the difference of demand charge, DoDC:

$$\text{DoDC} = \text{ODC}_{15-\text{min}} - \text{ODC}_{1-\text{hour}} \tag{4}$$

where $ODC_{15-\text{min}}$ and $ODC_{1-\text{hour}}$ are the optimal demand charge achieved using the same BESS and load profiles with 15 min and 1 hour time resolution, respectively. DoDC is a result of the peak difference caused by applying the BESS to a load with lower temporal resolution as compared to a load with higher temporal resolution. DoDC is hypothesized to depend on the BESS capacities – namely, power capacity, c_p, and energy capacity, c_e.

C. Battery space analysis

Given a specific load profile, the OP and corresponding ODC are determined by the BESS power and energy ratings. Due to human activity and equipment schedules, the load of a building varies based on the time of day. During the peak period(s), the BESS responds by supporting the load to limit grid imports once the power demand exceeds the OP. Since the SOC at the end of the day is constrained to be the same as at the beginning of the day, the BESS must recharge after each peak period. Hence, the BESS is able to reduce the peak by shifting demand, and its capacity ratings determine how much it can reduce the peak.

Several indicators characterize the load profile. The perfect peak, PP (kW), is the average

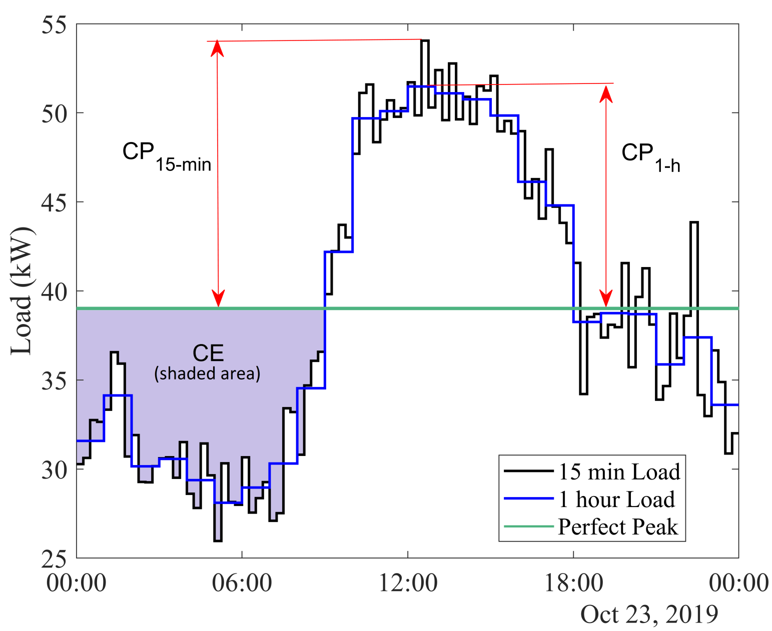

FIG. 2. 15 min and 1 hour temporal resolution load profiles, along with the perfect peak, on October 23, 2019. The maximum 15 min load occurs from 12:30 to 12:45 h at 54.05 kW, the maximum 60 min load occurs from 12:00 to 13:00 h at 51.48 kW, while the perfect peak is 39.02 kW (green line). The purple area shows the critical energy (Eq. 6a). The red lines show the critical power (Eq. 6b.)

power of the daily load:

$$PP = \frac{\sum_t^T l^t}{T} \tag{5}$$

A reduction of the load peak to the PP can only be achieved by a sufficiently large BESS. For a particular load profile, the BESS will have an ideal c_p and c_e, such that any larger capacity will not lower the optimal peak. These ideal capacities are defined as critical capacities— critical power, CP (kW), and critical energy, CE (kWh):

$$CP = \max|l^t - PP|, \quad \text{and} \tag{6a}$$

$$CE = 2 \times \max(|\sum_1^t [(l^t - PP) \times \Delta t]|) \tag{6b}$$

CP measures the maximum distance from the load to the PP at any time step. Because load profiles tend to be positively skewed, the positive maximum distance from the load is expected to be larger than the negative distance as shown in Fig. 2. $\mathrm{CP}_{15-\mathrm{min}}$ and $\mathrm{CP}_{1-\mathrm{hour}}$, describe the critical power for the 15 min and 1 hour temporal resolutions, respectively. It is intuitive – and confirmed in Fig. 2) – that the distance between the PP and extreme points in the 1 hour load is smaller than or equal to that of the 15 min load; thus, $CP_{1-\mathrm{hour}}$ is smaller than or equal to $CP_{15-\mathrm{min}}$. The overall CP is defined according to the 15 min timeseries, i.e. CP= $\mathrm{CP}_{15-\mathrm{min}}$. CE is twice the maximum absolute value of the cumulative sum of the distance from the 15 min load to the perfect peak for all time steps. This measures the minimum BESS energy capacity required to guarantee achieving the PP.

As the BESS capacities determine the OP for a particular load, we examine the variation of the DoDC with BESS energy and power capacities as the two dimensions of the battery ratings space (Fig. 3) The critical point is found at the intersection of the CP and CE lines. Note that the CP and CE change from day to day based on the load profile. To derive the DoDC across the battery rating space for the load profile of a particular day, each BESS candidate (i.e., every point in the battery rating space) is input to the optimization model. The DoDC is then calculated from the optimization results for the net load for both the 15 min and 1 hour temporal resolutions.

Based on the critical point, CE and CP, the battery rating space is divided into three regions (O), (P), and (E) in Fig. 3. BESS larger than the critical point in both power and energy (oversized region “O”) will have a DoDC of exactly zero. Once the BESS capacity exceeds CP and CE, the load at any temporal resolution equal to or larger than 15 min can be reshaped to the optimal result (the PP) and the additional battery capacities are not used. Hence, region (O) is named

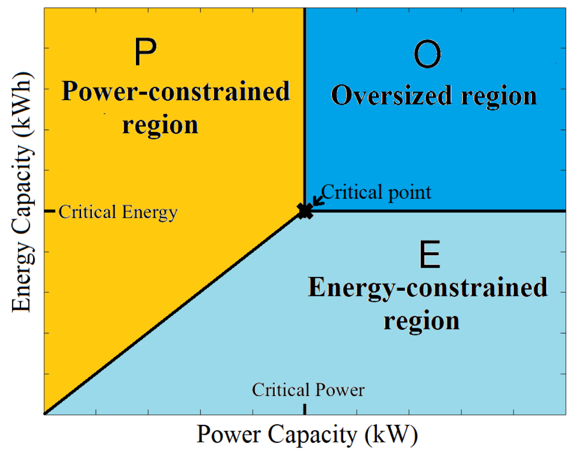

FIG. 3. Conceptual diagram of a typical battery ratings spaces consisting of "oversized" (O), "power-constrained" (P), and "energy-constrained" (E) regions.

the "oversized region", where the ODC for the load in both temporal resolutions are the same. BESSs with either power or energy capacity smaller than the critical point will not be able to reduce the peak to the PP for the load profiles in both resolutions. Then, the two OPs will differ, and the DoDC will not equal zero. In region (P), insufficient BESS power capacity restricts the peak shaving ability, while the energy capacity is sufficient. In region (P), if the power capacity is fixed while energy capacity increases, the two OPs and ODCs will not change because the power capacity limits the peak shaving performance. In region (E), insufficient BESS energy capacity restricts the peak shaving ability, while the power capacity is sufficient. Therefore, regions (P) and (E) are the "power-constrained region" and "energy-constrained region", respectively.

III. RESULTS AND DISCUSSION

A. Overview

Fig. 4a exemplifies the DoDC across the battery space based on the load on October 23. The ODC for the 15 min and 1 hour loads are shown respectively in Fig. 4b and Fig. 4c. The DoDC at each point in the battery space (Fig. 4a) is derived from the difference of the corresponding two ODCs (Fig. 4b and Fig. 4c). The two ODC plots confirm that the ODC is inversely proportional to the BESS power and energy capacities. The constant DoDC$=0$ region at the right top with large power and energy capacity, indicate that PP is achieved and both BESS power and energy capacity are larger than the critical point for both load profiles. Thus, the ODC is the same (i.e., ODC= \$804.52) at both temporal resolutions. At 15 min resolution, the reduction of ODC at the PP is \$309.99, or 27.81% of the maximum load, \$1114.51. The BESS achieves significant economic savings through demand charge management.

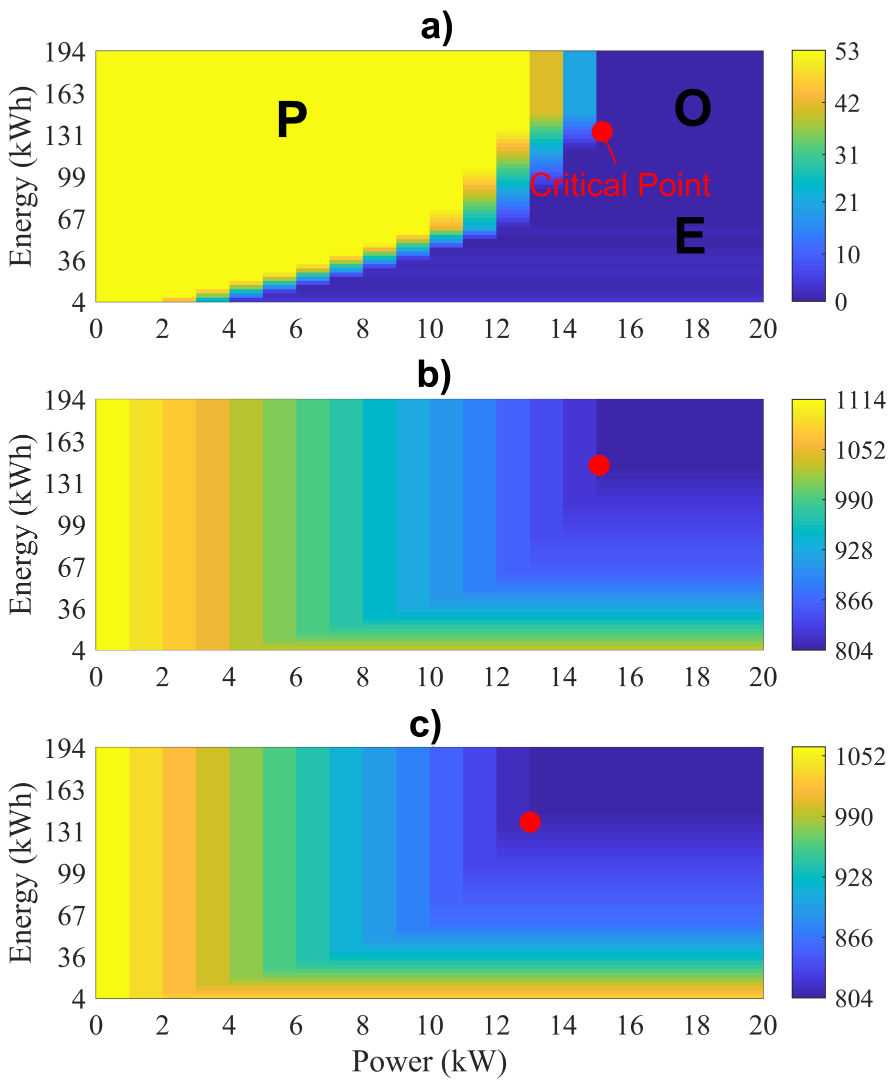

FIG. 4. Demand charge metrics (\$, color) for October 23 as a function of power and energy capacity: (a) DoDC, (b) ODC of 15 min load, and (c) ODC of 1 hour load. (a) is the difference between (b) and (c). The red circle shows the critical point. The regions in Fig. 3 are centered around the critical point in (a).

The distribution of DoDC in Fig. 4a is consistent with our conjectures about the optimal, power-constrained, and energy-constrained regions in Fig. 3. In the oversized region, DoDC is zero as expected. In the power-constrained region, DoDC is independent of energy capacity; in the energy-constrained region, DoDC is independent of power capacity. These findings confirm that 1 hour load profiles can overestimate peak shaving, as the DoDC values are non-negative across the battery ratings space. While the pattern in Fig. 4 is derived from the load profile on October 23, the generality is confirmed on other days (not shown). The battery space consisting of the critical point and three characteristic regions is the characteristic pattern of the DoDC for any load profile.

The meaning of the oversized region should be clear by now, but the two capacity-constrained regions still require further study. In Section III B, the power-constrained region is discussed, and peak shaving is quantified as a function of load averaging. In Section III C, the energy-constrained region is discussed, including a comparative analysis of the DoDC results from different days. Section III C also elucidates how the sequencing of 15 min load during the peak period affects the boundaries between the regions.

B. Power Constrained Region

To eliminate energy capacity constraints, the fixed energy capacity is chosen to be larger than the CE of the load profile, which is 146.84 kWh for October 23. For a randomly chosen fixed energy capacity of 175.41 kWh, DoDC, $\text{ODC}_{\text{15-min}}$ and $\text{ODC}_{\text{1-hour}}$ are shown in Fig. 5. Fig. 5 represents a horizontal slice of the battery ratings space at $c_e = 175.41$ kWh in Fig. 4a. The left side, marked as (P), represents the power-constrained region, while the right side, (O), represents the oversized region. The two sides are split by the CP. As the battery power capacity increases, $\text{ODC}_{\text{15-min}}$ and $\text{ODC}_{\text{1-hour}}$, decrease linearly and in parallel with a fixed difference of \$52.99, starting from \$1114.51 and \$1061.52 respectively. This trend remains until the power capacity reaches the CP, after which both ODCs settle at the same level. The DoDC is constant until the power capacity reaches 12.46 kW (CP_{1-h}), where DoDC falls rapidly before settling at zero for a power capacity of 15.03 kW (CP_{15-min}).

The ODC in the power-constrained region is affected by time averaging of the load from high-resolution (15 min) to low-resolution (1 hour). The constant DoDC of \$52.99 for power ratings smaller than the transient zone in Fig. 5 results from

$$(\mathrm{ML}_{15-\mathrm{min}} - \mathrm{ML}_{1-\mathrm{hour}}) \times \mathrm{d} = \$52.99 \tag{7}$$

where $\text{ML}_{\text{15-min}}$= 54.05 kW and $\text{ML}_{\text{1-hour}}$= 51.48 kW are the maximum load demand of October 23 for the two time resolutions. For example, Fig. 6a displays the loads and net loads

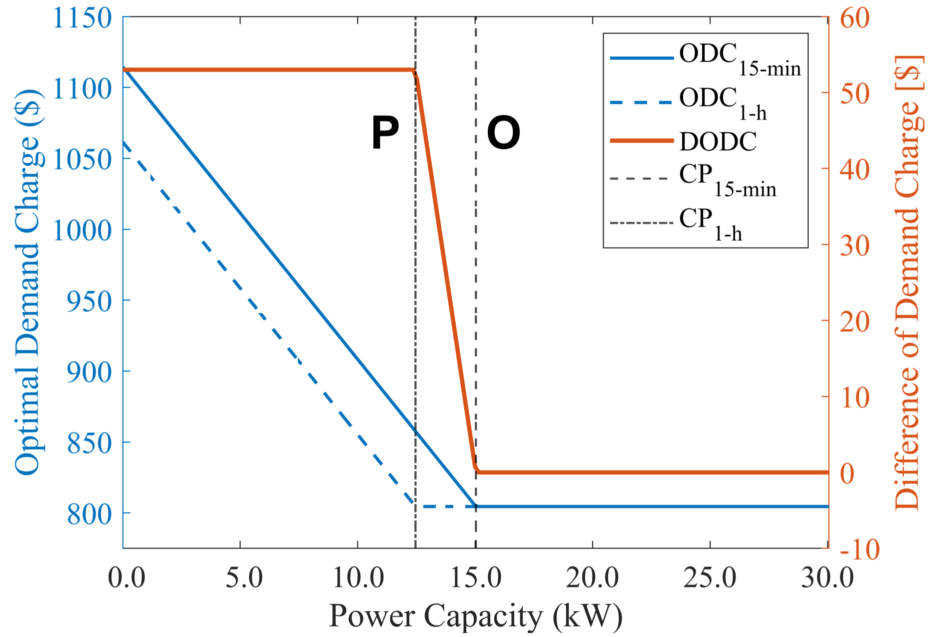

FIG. 5. DoDC, $\mathrm{ODC}_{\text{15-min}}$, and $\mathrm{ODC}_{\text{1-hour}}$ on Oct 23 at a fixed BESS energy capacity of 175.41 kWh.

as optimized by the same BESS energy capacity as in Fig. 5 in the power-constrained region. $\mathrm{M}_{\text{15-min}}$= 45.65 kW occurs at 12:30 to 12:45 h while $\mathrm{ML}_{\text{1-hour}}$= 43.08 kW occurs at 12:00 to 13:00 h. The difference of 2.57 kW results in DoDC = $52.99 for the day.

The sharp drop in DoDC occurs between the CPs of the loads for the two temporal resolutions. Hence, the two CPs marks the transient zone between the power-constrained and the oversized regions. The beginning and end of the transient DoDC zone, 12.46 kW and 15.03 kW, occur at CP of the 1 hour and 15 min load, $\mathrm{CP}_{\text{1-hour}}$=12.46 kW and $\mathrm{CP}_{\text{15-min}}$=15.03 kW for October 23. The difference of the two CPs is caused by time averaging. Fig. 6b displays the optimization results of a BESS with capacity of $c_p = \mathrm{CP}_{\text{1-hour}}$ and large energy capacity. With a power capacity of $\mathrm{CP}_{\text{1-hour}}$, the 1 hour net load becomes flat and equal to the PP of 39.02 kW. However, the $\mathrm{CP}_{\text{1-hour}}$ BESS is unable to completely flatten the 15 min load, resulting in a net load peak of 41.59 kW during 12:30 to 12:45 h. The 2.57 kW increase over the PP results in a DoDC= $52.99 in Fig. 5.

In the power-constrained region, the peak shaving depends solely on two factors: the peak demand (maximum load in kW) and the power capacity of the BESS. The energy capacity will not constrain the peak shaving (i.e. the BESS will not discharge to zero SOC), but the power capacity of the BESS will be fully utilized at the time interval with the peak demand. The original peak difference between the two load profiles is maintained, as the limited power capacity of the BESS

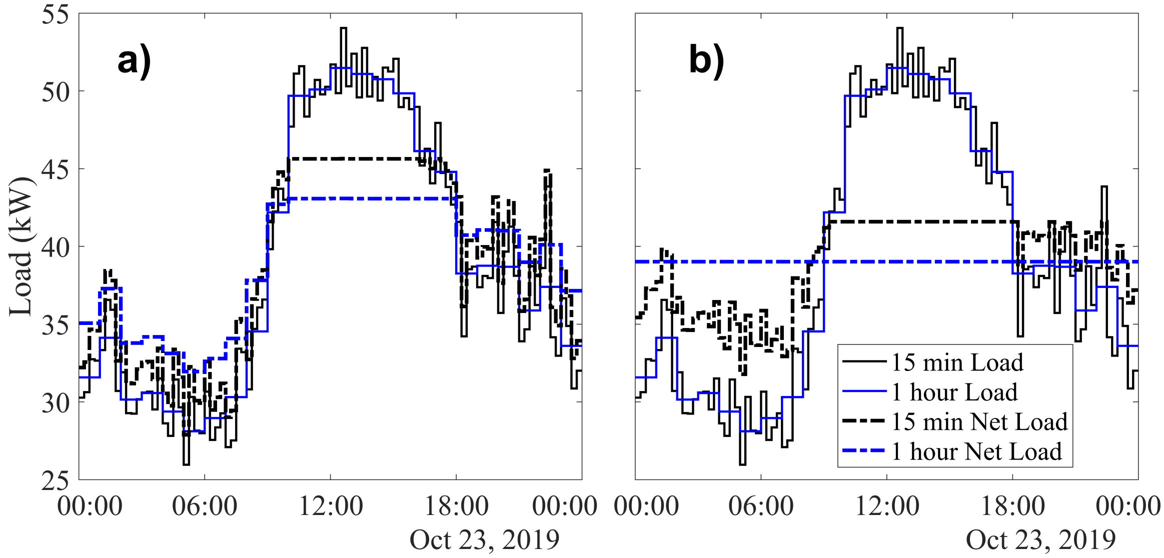

FIG. 6. 15 min and 1 hour load on October 23 and net load optimized for the following BESS: a) 8.40 kW, 175.41 kWh; b) 12.46 kW (= $CP_{\text{1-hour}}$) and 175.41 kWh.

is unable to reduce the peak demand to the PP. Even when the energy capacity is smaller than at the critical point, there will be a range (i.e., the lower power-constrained region in Figs. 3 and 3) where peak shaving is limited by the power capacity, thus maintaining the original peak difference.

C. Energy Constrained Region

1. Three example days: Overview

To analyze the DoDC in the energy-constrained region, the power capacity is fixed at the CP. Fig. 7 presents the variation of the $ODC_{\text{15-min}}$, $ODC_{\text{1-hour}}$, and the corresponding DoDC for Oct 7 (CP = 10.20 kW), Oct 13 (CP = 16.40 kW), and Oct 23 (CP = 15.03 kW). Selecting a fixed power capacity of CP eliminates the potential influence of insufficient power, ensuring that the effect of constrained energy capacity can be analyzed in isolation. In Fig. 7, the left (E) part represents the energy-constrained region, while the right (O) part represents the oversized region. The DoDC at zero energy capacity is the same as the DoDC in the power-constrained region (and the DoDC of the original load), but DoDC decreases rapidly as the energy capacity increases. For c_e0, the ODCs at both time resolutions are closer to each other, as compared to the ODCs in the power-constrained region in Fig. 5, resulting in a small DoDC magnitude of a few \$. However, the

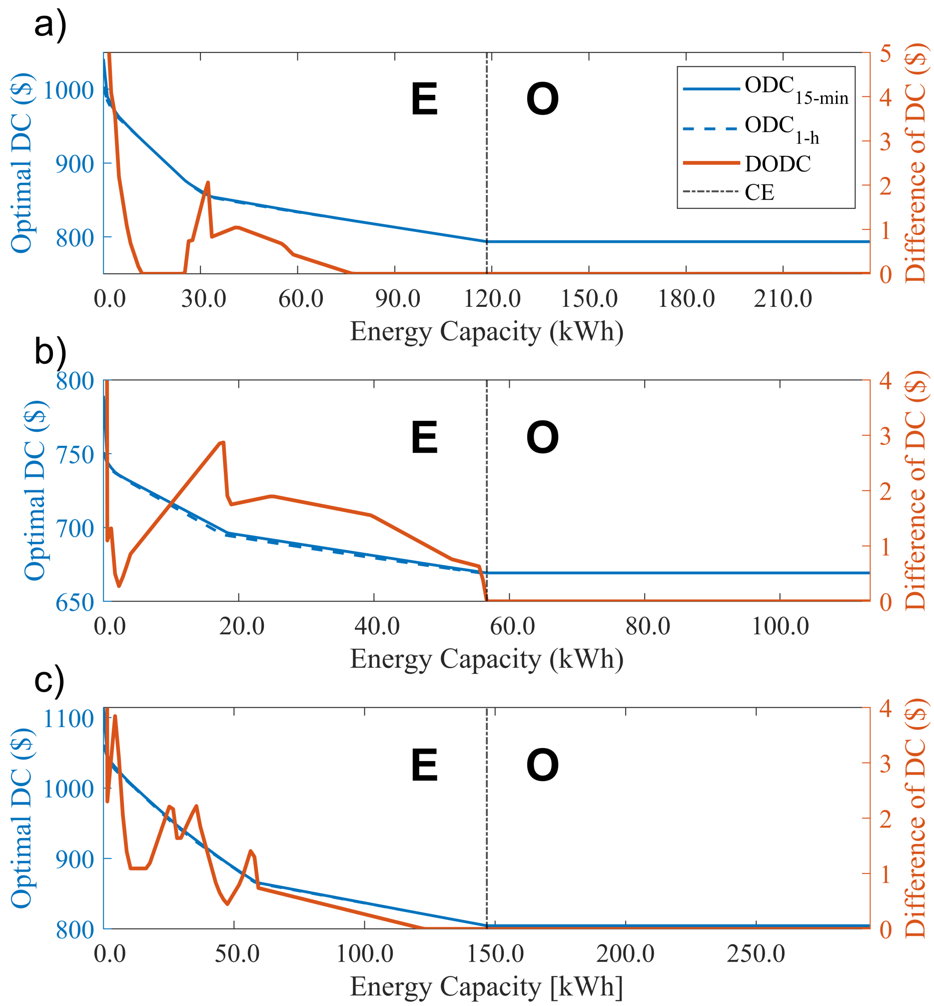

FIG. 7. The DoDC at the critical power capacity as a function of BESS energy capacity for a) Oct 7, b) Oct 13, and c) Oct 23. (O) represents the oversized region and (E) represents the energy-constrained region. The vertical dashed line represents the critical energy (CE).

variation of the DoDC in the energy-constrained region is more complex and irregular than in the power-constrained region.

The energy-constrained regions of Oct 7 and Oct 23 show that the DoDC reaches zero at some energy capacity smaller than CE. For Oct 7, DoDC$=0$ when $11.97 < c_e < 25.10$ kWh & $c_e > 76.58$ kWh (Fig. 7a) and for Oct 23, DoDC$=0$ for $c_e > 123.10$ kWh (Fig. 7c). However, this feature is inconsistent, as DoDC$\neq 0$ in the energy-constrained region for Oct 13 and the DoDC behavior for Oct 7 and 23 differs. The reason for the inconsistent results is a change in the peak period duration of some load profiles for the original versus the time-averaged load. For other load profiles, where the averaging does not change the peak period duration, DoDC$=0$ at CE as

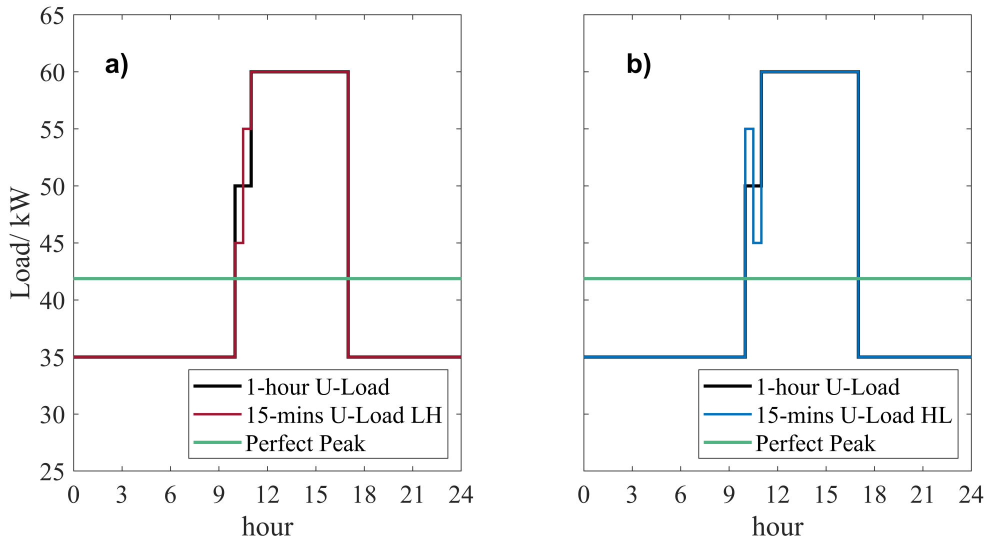

FIG. 8. Artificial load profiles at 15 min and averaged to 1 hour resolution: a) Sequence LH, and b) Sequence HL.

expected based on the definition of CE. We demonstrate this "sequence effect" through artificial load profiles and then verify the conclusion using real data from Oct 7.

2. Artificial load and sequencing

To illustrate the impact of the load sequence on DoDC in the 15 min profile, a regular inverse U-shaped load with a flat peak demand from 1100 to 1700 h is employed. In Fig. 8, the two 15 min resolution load profiles are identical except during the beginning of the peak period (1000–1100 h). During 1000-1100 h the hourly average is identical, but the 15 min profiles differ. As shown in Table 1, the four power demands from 1000-1100 h have the same values but are arranged in a different order; in other words, the sequence differs. Sequence LH (low-high) starts with smaller loads of 45 kW from 1000-1030 h and ends with higher loads of 55 kW from 1030-1100 h; sequence HL (high-low) is the reverse.

Since the three artificial loads (i.e., the two 15 min profiles and the 1 hour profile) have identical peak loads, the net load peak is not affected by the power capacity of the BESS. However, the 15 min load sequence at the start of the load peak (e.g., 1000 to 1100 h) changes the peak duration. An energy-constrained BESS, with power capacity of 25 kW and energy capacity of 45 kWh, is selected for the net load peak optimization (Fig. 9). The CP for Sequence LH

TABLE I. Data of the artificial load time series shown in Fig. 8. The three load profiles share the same CP of 20.2 kW and the same CE of 195.8 kWh

	Load Profile / kW			
	0:00-10:00	10:00-11:00	11:00-17:00	17:00-24:00
1-hour	35	50,50,50,50	60	35
15-min Sequence LH	35	45,45,55,55	60	35
15-min Sequence HL	35	55,55,45,45	60	35

(CP= 52.69 kW) is 0.19 kW higher than for Sequence HL (CP= 52.50 kW) and for the 1-hour average (CP= 52.50 kW). Though this difference is small, it is of fundamental interest because the DoDC changes from zero to non-zero as a result of a seemingly irrelevant modification from Sequence LH to Sequence HL.

As the BESS energy is sized to achieve an optimal net load between 50 kW and 55 kW, the start of the peak period of the 1 hour load and sequence HL is at 1100 h, while the start in sequence LH is at 1030 h due to its step-shaped peak demand period. This difference in the start time of the peak period also manifests in the SOC, where the discharging period starts at 1030 h for sequence LH but at 11:00 h for sequence HL and the 1 hour averaged load. Therefore, a BESS with a limited energy capacity can achieve a lower net load peak for the 1 hour averaged load than for Sequence LH. On the other hand, Sequence HL has a recharging period of 1030-1100 h, allowing the BESS SOC to recover after discharging from 1000 to 1030. This recovery more efficiently uses the limited energy capacity, as the net effect of the sequence HL in 1000-1100 h is the same as for the aggregated 1 hour U-load. Subsequently, the 1 hour Load and sequence HL have identical optimal peaks.

In summary, a difference in sequence in the 15 min load can affect the optimal net-load peak. In this example, the 15 min sequence in the beginning of the peak period has a lower demand followed by a higher demand with an identical hourly average. The result is an increased optimal net-load peak, as compared to the corresponding 1 hour load. This occurs because the duration of the peak period is extended, and the integral between the target peak net load and the original load then contains more energy that cannot be shaved by a BESS with limited energy capacity. Note that the energy sequence during the original load peak period is irrelevant, as it does not extend the duration of the peak period. However, the energy sequence at the end of the peak period

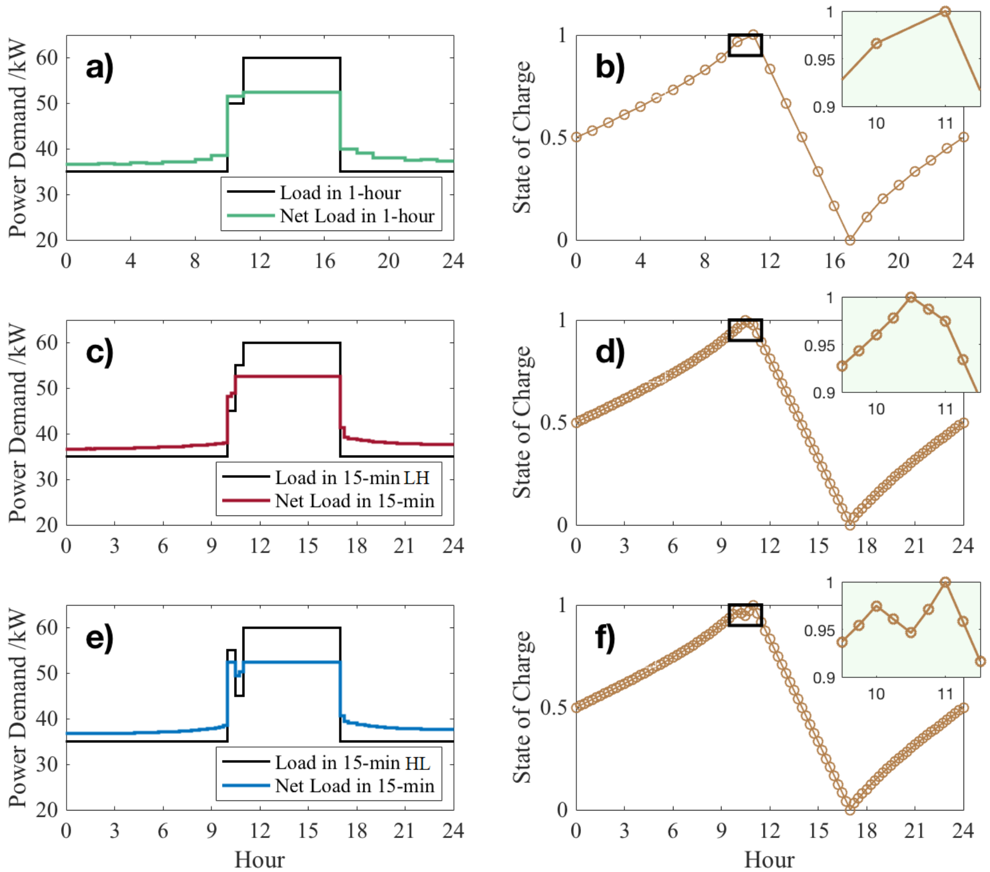

FIG. 9. a, b) 1 hour artificial load of Table I and its optimized net load and SOC by an energy-constrained battery. c, d) Load, net load, and SOC of the 15 min load in sequence LH. e, f) Load, net load and SOC of the 15 min load in sequence HL.

also affects the optimal peak: a decreasing trend in the 15 min energy sequence will increase the optimal peak, while an increasing trend will result in zero DoDC.

3. *Sequence Verification on Oct 7*

To verify the energy sequence effect conclusions from the artificial data, a modified 15 min load from Oct 7 is designed and the corresponding battery space is studied. According to the original DoDC results in Fig. 7 and the load in Fig. 10, for *OP*45 kW the peak period starts at 1300 h and ends at 1800 h. For 40 kWOP45 kW, the peak period starts as early as 0900 h and extends to as late as 2300 h. Following the analysis in Section III C 2, we can achieve optimal net load peak equality between 15 min and 1 hour loads by re-ordering the energy sequence within

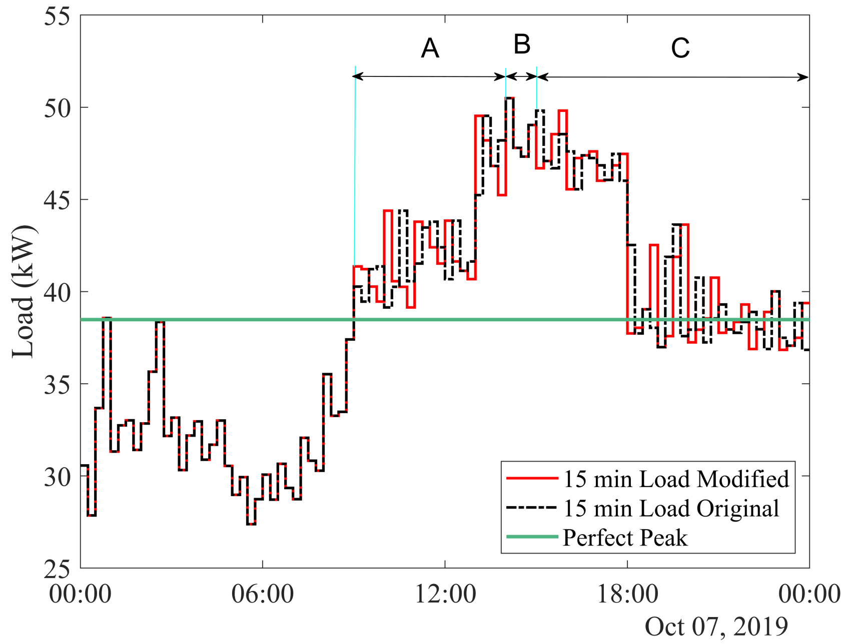

FIG. 10. Original and modified load profile on Oct 7. The duration when the peak load within the hour is greater than the OP is divided into three regions: A) before peak load hour: load is reordered in descending order; B) peak-load hour: load is left unchanged; and C) after peak-load hour (C): load is reordered in ascending order.

these specified hours. During the beginning of the peak period (before 1400 h), the four 15 min periods within each hour are reordered from largest to smallest and the opposite sequencing is applied at the end of the peak period as show in see Fig. 10. The modified load shares the same 1 hour averages, CE, and CP as the original load. A slice across the energy-constrained region at CP based on the optimization result for the DoDC of the modified Oct 7 load is shown in Fig. 11. The DoDC in the entire energy-constrained regions is now zero (except the trivial situation when $c_e = 0$), supporting our hypothesis about the sequence effect.

In summary, time averaging can affect the duration of the peak period based on the particular time sequence of the 15 min loads. Therefore, for energy-constrained BESS, time averaging the load can result in an underestimation of ODC for the net load.

IV. CONCLUSIONS

A. Summary

In this paper, the difference of optimal demand charge (DoDC) derived from net load peak minimization of load data at two temporal resolutions (i.e., 15 min and 1 hour) is analyzed for a range of battery power and energy ratings. The battery rating space can be divided into three characteristic regions. A 1-hour averaged load may overestimate peak shaving potential for batteries with limited power or energy capacities. Specifically, in the power-constrained region of the battery rating space, the difference between the original (15 min) and the 1 hour average load peak persists in the optimized net load until the battery power capacity is sufficiently large. In the energy-constrained region, averaging can change the peak period duration for increasing (decreasing) sub-hourly sequence of the original load data right before (after) the peak period. Through artificial load data and reordering of real load data, we demonstrated that the sequence effect causes energy-constrained batteries to underestimate peak shaving.

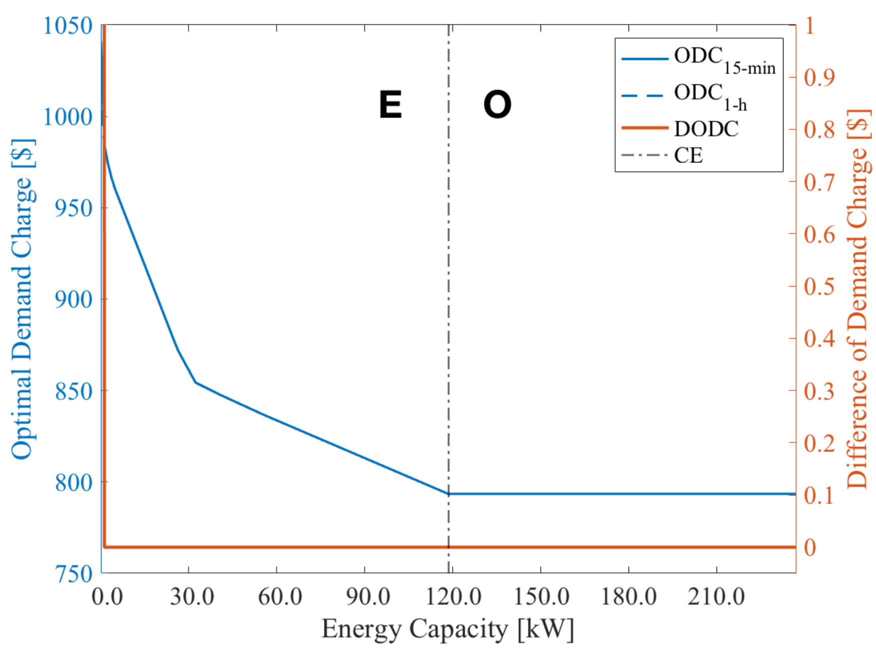

FIG. 11. The DoDC for the critical power capacity for the modified load of October 7 as a function of the BESS energy capacity. (E) represents the energy-constrained region and (O) represents the oversized region. Compared to Fig. 7a, DoDC is now zero throughout for non-zero energy capacities.

B. Discussion of assumptions and limitations

The conclusions derived from the load data of one-day periods apply to demand charge analysis of a month, or even a whole year, because the peak load of a time period longer than a single day varies based on the most challenging day(s) within the period (i.e., the days with largest critical power (CP) or critical energy (CE)). For load profiles with a "spiky" peak caused by short peak duration (i.e., high CP, low CE), the overestimation of optimal demand charges for loads at low temporal resolution tends to be high for a BESS in the power-constrained region. On the other hand, for load profiles with a "broad" peak (i.e., low CP, high CE), the DoDC is relatively more expressed for batteries with limited energy capacity, and thus the energy-constrained region would be larger.

In this paper, 15-min and 1-hour intervals are chosen for comparison as high- and low-resolution, respectively. However, the analysis and conclusions also apply for other temporal resolutions.

The assumptions detailed at the end of the introduction and the beginning of Section II.A cause the results to be idealized. Considering capacity limitations of converters and electrical lines would make some of the analyses infeasible, but does not affect the structure of the battery rating space. Considering losses in transformation, conversion, conduction, and storage of electric power and energy would mainly increase energy use, but only minimally increase peak demand and demand charges. Losses would be expected to impact 15 min and 1 hour loads similarly and therefore not affect the DoDC battery ratings space. The effect of adding peak demand charges and time-of-use charges will be studied in a future paper.

Using real (instead of perfect) forecasts would be expected to increase the DoDC as forecast errors tend to increase with the variability of the timeseries which is higher for 15 min than 1 hour loads. Larger forecast errors can result in premature battery discharge or in sub-optimal intra-15 min scheduling that increase peak demand. As a result the oversized region would be expected to shrink, i.e. start at a power rating and energy rating larger than the CP and CE, respectively.

C. Significance

The concept of partitioning the BESS ratings space offers a new perspective for the study of BESS demand charge reduction at different temporal resolutions. The details of high-resolution

TABLE II. Summary of DoDC for three days. For the energy constrained region, only $c_e > 10$ kWh is considered.

Day	15-min peak load (kW)	Max DoDC ($)	
		Power constrained	Energy constrained
Oct 7	50.49	37.73	2.06
Oct 13	38.28	38.35	2.87
Oct 23	54.05	52.99	2.22

profiles should be considered carefully in demand side management for a BESS with limited capacities. Capturing actual peak demand at the time resolution consistent with the utility tariff (here 15 min) is especially critical for the BESS economics, but temporal sequencing of the load can also cause a small overestimation of demand charge reduction for time averaged load data. Anecdotally, Table II shows that differences in demand charge for the three days simulated were $37 to $53 per day for a power-constrained battery and $2 to $3 per day for an energy constrained battery. In practice, choosing a BESS with larger power and energy capacities than those determined from optimization at low temporal resolution can offset the DoDC uncertainties from load resolution conversion. Our results show that demand charge savings can be especially sensitive to the BESS power capacity; therefore the power capacity of the battery should be carefully considered when interpreting results from optimizations at low resolutions. Conversely, if the 15 min (net) load data are available and the modeling tool restricted the temporal resolution to 1 hour, DoDC can be mitigated by up-sizing the BESS from $\mathrm{CP}_{1-\mathrm{h}}$ to $\mathrm{CP}_{15-\mathrm{min}}$ (see Fig. 5).

Depressed solar energy production can cause large net load peaks. The largest net load peaks often occur, when heavy rain associated with thunderstorms depresses solar energy production by up to 90%, yet thunderstorms are short-lived and their largest impact may not the represented in hourly data. Therefore, underestimation of demand charge savings for hourly net load profiles would likely be larger for sites with solar energy production compared to what was observed in this paper.

In Burgio et al.[18] the peak of the 15 min load, 15 min load+PV, and 15 min PVB grid imports was 12%, 15%, and 15% higher than that of hourly load for one day, respectively. For Oct 23 in our paper, the 15-min load peak (54.1 kW) was 4.8% or 2.6 kW higher than the hourly load (51.5 kW). Our analysis shows how BESSs of different energy and power ratings reduce the difference in the peak net load, which is equivalent to the PVB peak in Burgio et al. The peak net load difference is completely eliminated by a BESS in the optimal region and mostly eliminated by a BESS in the energy constrained region (less than a \$2.2 or 0.1 kW difference). BESS in the power constrained region (up to a power rating of about 13 kW) do not reduce the net load difference, unless the BESS energy rating is large enough to place the BESS to the right of a line of about $c_e = 0.2c_p 1$ h in the battery rating space. Our analysis shows that the ability of a given BESS system to reduce the net load difference is driven by the variability in the original load shape, in particular the critical power and critical energy.

This comprehensive study of the effect of temporal resolutions on peak shaving provides novel insights into how load profiles interact with BESS power and energy ratings to determine peak shaving effectiveness.

DATA AVAILABILITY STATEMENT

This paper uses the building load data of the Police Department of UC San Diego. The load data was released publicly in an earlier publication[21].

REFERENCES

[1]A. Nottrott, J. Kleissl, and B. Washom, "Energy dispatch schedule optimization and cost benefit analysis for grid-connected, photovoltaic-battery storage systems," Renewable Energy **55**, 230 – 240 (2013).

[2]H. Chen, T. N. Cong, W. Yang, C. Tan, Y. Li, and Y. Ding, "Progress in electrical energy storage system: A critical review," Progress in Natural Science: Materials International **19**, 291–312 (2009).

[3]J. Leadbetter and L. Swan, "Battery storage system for residential electricity peak demand shaving," Energy and Buildings **55**, 685 – 692 (2012), cool Roofs, Cool Pavements, Cool Cities, and Cool World.

[4]M. Stadler, H. Aki, R. M. Firestone, J. Lai, C. Marnay, and A. S. Siddiqui, "Distributed energy resources on-site optimization for commercial buildings with electric and thermal storage technologies," in *2008 ACEEE Summer Study on Energy Efficiency in Buildings, Scaling Up: Building Tomorrow's Solutions, August 17-22, 2008*, LBNL (LBNL, Pacific Grove, CA, 2008).

[5]K. Anderson, D. Cutler, E. Elgqvist, D. Olis, H. Walker, N. Laws, N. DiOrio, S. Mishra, J. Pohl, K. Krah, *et al.*, "Reopt lite™," Tech. Rep. (National Renewable Energy Lab.(NREL), Golden, CO (United States), 2019).

[6]J. E. Bistline, "The importance of temporal resolution in modeling deep decarbonization of the electric power sector," Environmental Research Letters **16**, 084005 (2021).

[7]K. Abdulla, K. Steer, A. Wirth, J. De Hoog, and S. Halgamuge, "The importance of temporal resolution in evaluating residential energy storage," in *2017 IEEE Power & Energy Society General Meeting* (IEEE, 2017) pp. 1–5.

[8]K. Poncelet, E. Delarue, J. Duerinck, D. Six, and W. D'haeseleer, "Impact of temporal and operational detail in energy-system planning models," URL https://www. mech. kuleuven. be/en/tme/research/energy_environment/Pdf/wp-en201420-2. pdf.

[9]M. Jaszczur, Q. Hassan, and J. Teneta, "Temporal load resolution impact on pv/grid system energy flows," in *MATEC web of conferences*, Vol. 240 (EDP Sciences, 2018) p. 04003.

[10]F. Schmid, J. Winzer, A. Pasemann, and F. Behrendt, "An open-source modeling tool for multi-objective optimization of renewable nano/micro-off-grid power supply system: Influence of temporal resolution, simulation period, and location," Energy **219**, 119545 (2021).

[11] B. Hauck, W. Wang, and Y. Xue, "On the model granularity and temporal resolution of residential pv-battery system simulation," Developments in the Built Environment **6**, 100046 (2021).

[12] R. Tang, K. Abdulla, P. H. Leong, A. Vassallo, and J. Dore, "Impacts of temporal resolution and system efficiency on pv battery system optimisation," in *2017 Asia-Pacific Sol. Res. Conf* (2017).

[13] H. Yang, Y. Zhang, Y. Ma, M. Zhou, and X. Yang, "Reliability evaluation of power systems in the presence of energy storage system as demand management resource," International Journal of Electrical Power & Energy Systems **110**, 1–10 (2019).

[14] A. Wright and S. Firth, "The nature of domestic electricity-loads and effects of time averaging on statistics and on-site generation calculations," Applied Energy **84**, 389 – 403 (2007).

[15] S. Cao and K. Sirén, "Impact of simulation time-resolution on the matching of pv production and household electric demand," Applied Energy **128**, 192–208 (2014).

[16] P. Stenzel, J. Linssen, J. Fleer, and F. Busch, "Impact of temporal resolution of supply and demand profiles on the design of photovoltaic battery systems for increased self-consumption," in *2016 IEEE International Energy Conference (ENERGYCON)* (2016) pp. 1–6.

[17] T. Beck, H. Kondziella, G. Huard, and T. Bruckner, "Assessing the influence of the temporal resolution of electrical load and pv generation profiles on self-consumption and sizing of pv-battery systems," Applied Energy **173**, 331 – 342 (2016).

[18] A. Burgio, D. Menniti, N. Sorrentino, A. Pinnarelli, and Z. Leonowicz, "Influence and impact of data averaging and temporal resolution on the assessment of energetic, economic and technical issues of hybrid photovoltaic-battery systems," Energies **13**, 354 (2020).

[19] D. Talavera, F. Muñoz-Rodriguez, G. Jimenez-Castillo, and C. Rus-Casas, "A new approach to sizing the photovoltaic generator in self-consumption systems based on cost–competitiveness, maximizing direct self-consumption," Renewable energy **130**, 1021–1035 (2019).

[20] O. Babacan, A. Abdulla, R. Hanna, J. Kleissl, and D. G. Victor, "Unintended effects of residential energy storage on emissions from the electric power system," Environmental science & technology **52**, 13600–13608 (2018).

[21] S. Silwal, C. Mullican, Y.-A. Chen, A. Ghosh, J. Dilliott, and J. Kleissl, "Open-source multi-year power generation, consumption, and storage data in a microgrid," Journal of Renewable and Sustainable Energy **13**, 025301 (2021).